A mesoscopical model of shape memory alloys

Tomáš Roubíček[a,b], Martin Kružík[b,c], and Jan Koutný[b]

[a] Mathematical Institute, Charles University, Sokolovská 83, CZ-186 75 Praha 8, Czech Republic; tomas.roubicek@mff.cuni.cz
[b] Institute of Information Theory and Automation, Academy of Sciences of the Czech Republic, Pod vodárenskou věží 4, CZ-182 08 Praha 8, Czech Republic; kruzik@utia.cas.cz, koutny@utia.cas.cz
[c] Department of Physics, Faculty of Civil Engineering, Czech Technical University, Thákurova 7, CZ-16629 Praha 6, Czech Republic

Abstract. Multiwell stored energy related to austenite and particular martensitic variants as well as a dissipation pseudopotential are used to assembly a mesoscopical model for an isothermal rate-independent martensitic transformation in shape memory alloys. Theoretical results concerning numerical approximation of involved Young measures by laminates are surveyed and computational experiments are presented for CuAlNi single crystals.

Key words: martensitic transformation, rate-independent processes, Young measures.

1. INTRODUCTION, STORED ENERGY, MICROSTRUCTURE, DISSIPATION ENERGY

Shape memory alloys (SMAs) belong to the so-called smart materials which enjoy important applications. These exhibit specific, *hysteretic* stress/strain/ temperature response and a so-called *shape memory effect*. The mechanism behind it is quite simple: atoms tend to be arranged in several crystallographical configurations having different symmetry groups: higher symmetrical one (referred to as the *austenite* phase, typically cubic) has higher thermal capacity while lower symmetrical one (called the *martensite* phase, typically tetragonal, orthorhombic, or monoclinic) has lower thermal capacity and may exist, by symmetry, in several variants (typically 3, 6, or 12, respectively). We refer to [1−7] for a thorough survey. Here we consider only isothermal stress–strain response modelling.

We consider a bounded Lipschitz domain $\Omega \subset \mathbb{R}^3$ as a reference configuration (canonically the stress-free austenite). Standardly, the *displacement* $u : \Omega \to \mathbb{R}^3$ and the *deformation* $y : \Omega \to \mathbb{R}^3$ are related by $y(x) = x + u(x)$, $x \in \Omega$. Hence the *deformation gradient* is $F = \nabla y = \mathbb{I} + \nabla u$, where $\mathbb{I} \in \mathbb{R}^{3\times3}$ denotes the identity matrix. Mechanical response is phenomenologically described by a specific *stored energy* $\widehat{\varphi} = \widehat{\varphi}(F)$, assumed to have a *p*-polynomial growth/coercivity structure. The *frame-indifference*, i.e. $\widehat{\varphi}(F) = \widehat{\varphi}(RF)$ for any $R \in \mathrm{SO}(3)$, the group of orientation-preserving rotations, requires that $\widehat{\varphi}(\cdot)$ in fact depends only on the (right) Cauchy–Green stretch tensor $C := F^\mathrm{T} F$. We abbreviate

$$\varphi(\cdot) := \widehat{\varphi}(\mathbb{I} + \cdot\,). \tag{1}$$

The overall free energy related to a displacement profile u is $\Phi(u) := \int_\Omega \varphi(\nabla u)\mathrm{d}x$. Considering a (time-varying) elastic support $w(t,x)$ on a part Γ of the boundary $\partial\Omega$, we expand it to the stored energy $G(t,u) = \Phi(u) + \frac{1}{2} \int_\Gamma (u - w(t,\cdot))^\top B(u - w(t,\cdot))\mathrm{d}S$ with $B^\top = B$. Due to the multiwell character of φ, the deformation gradient usually tends to develop fast spatial oscillations if it tends to minimize the overall stored energy under given boundary conditions, see [1,4,8,9], resulting in a *microstructure* that can effectively be described by so-called *gradient Young measures*, which are measurably parameterized probability measures $x \mapsto \nu_x$ on $\mathbb{R}^{3\times3}$ that can be attained by gradients in the sense $\lim_{k\to\infty} \int_\Omega g(x)v(\nabla u_k(x))\,\mathrm{d}x = \int_\Omega g(x) \int_{\mathbb{R}^{3\times3}} v(A)\,\nu_x(\mathrm{d}A)\mathrm{d}x$ for some sequence $\{u_k\}_{k\in\mathbb{N}} \subset W^{1,p}(\Omega;\mathbb{R}^3)$ and all $g \in L^\infty(\Omega)$ and $v \in C_0(\mathbb{R}^{3\times3})$, see [9]; the notation C_0, L^p, $W^{1,p}$ for function spaces is standard. Let us denote the set of all such parameterized measures by $\mathcal{G}^p(\Omega;\mathbb{R}^{3\times3})$. The continuously extended (so-called *relaxed*) stored energy is then

$$\bar{G}(t,u,\nu) = \int_\Omega \int_{\mathbb{R}^{3\times3}} \varphi(A)\,\nu_x(\mathrm{d}A)\mathrm{d}x + \int_\Gamma \frac{(u - w(t,\cdot))^\top B(u - w(t,\cdot))}{2}\,\mathrm{d}S. \tag{2}$$

The pair of "macroscopical" displacement u and the gradient Young measures ν represents a quite natural *mesoscopical description* of the state of the body. The "kinematically" admissible pairs (u,ν) are in

$$Q := \left\{ (u,\nu) \in W^{1,p}(\Omega;\mathbb{R}^3) \times G^p(\Omega;\mathbb{R}^{3\times3}); \int_{\mathbb{R}^{3\times3}} A\nu_x(\mathrm{d}A) = \nabla u(x) \text{ for a.a. } x \right\}.$$

Within microstructure evolution due to time-varying loading w, SMAs *dissipate energy*. For sufficiently slow loading, these processes are *activated* and quite *rate-independent*, leading to a *hysteretic* stress–strain response. We assume dissipative forces having a (pseudo)potential, say R, and that the energy dissipated during the phase-transformation process depends (counting phenomenologically, beside possible rank-one connections, with various impurities) on the starting and final (phase) variants, only; this (simplifying) concept has been adopted also in [10–14]. We implement this philosophy with the help of a frame-invariant "phase indicator" being a smooth bounded function $\hat{\mathcal{L}} : \mathbb{R}^{3\times3} \to \mathbb{R}^L$, with L denoting the

number of (phase) variants. Then, with $\mathcal{L}(A) := \hat{\mathcal{L}}(\mathbb{I} + A)$ like (1), the dissipation potential is postulated as

$$R(\nu) := \int_{\Omega} \delta_K^*(\lambda(x)) \, \mathrm{d}x \quad \text{with} \quad \lambda(x) = \int_{\mathbb{R}^{3 \times 3}} \mathcal{L}(A) \, \nu_x(\mathrm{d}A)\mathrm{d}x, \qquad (3)$$

with a convex compact $K \subset \mathbb{R}^L$ determining the *activation stresses*, δ_K being its indicator function, and δ_K^* its conjugate which is, of course, homogeneous degree-1. The quantity λ plays the role of a macroscopic *volume fraction* assigned through (3) to the microstructure described by ν.

2. ENERGETIC SOLUTION, LAMINATES, NUMERICAL APPROXIMATION

With neglecting kinetic energy and based on the *minimum-stored-energy principle* competing with the *maximum-dissipation* (or rather *realizability* [15]) *principle*, in the scalar (hence convex) case, the desired evolution $(u, \nu) = (u(t), \nu(t)) : [0, T] \to Q$ would be governed by the doubly-nonlinear evolution inclusion

$$\begin{pmatrix} 0 & 0 \\ 0 & \partial R(\frac{\mathrm{d}\nu}{\mathrm{d}t}) \end{pmatrix} + \partial_{(u,\nu)}\big[\bar{G} + \delta_Q\big](t, u, \nu) \ni 0 \quad \text{for } t \in [0, T], \qquad (4)$$

considered completed by an initial condition, here on λ. In the convex case, it is equivalent (see [16,17]) to the *energetic formulation*, i.e. *stability*

$$\forall (\tilde{u}, \tilde{\nu}) \in Q : \quad \bar{G}\big(t, u(t), \nu(t)\big) \leq \bar{G}(t, \tilde{u}, \tilde{\nu}) + R\big(\nu(t) - \tilde{\nu}\big), \qquad (5)$$

together with the *energy equality*

$$\mathfrak{G}(t) + \mathrm{Var}_R(\nu; s, t) = \mathfrak{G}(s) - \int_{(s,t) \times \Gamma} (u - w)^{\top} B \frac{\partial w}{\partial t} \, \mathrm{d}S\mathrm{d}t \qquad (6)$$

to be satisfied for any $0 \leq s < t \leq T$, where $\mathfrak{G}(t) := \bar{G}(t, u(t), \nu(t))$ is the Gibbs energy and $\mathrm{Var}_R(\nu; s, t)$ denotes the total variation over $[s, t]$ of $\nu(\cdot)$ with respect to R from (3). The particular terms in (6) represent the stored energy at time t, the energy dissipated by changes of the internal structure during the time interval $[s, t]$, the stored energy at the initial time s, and work done by external loadings during the time interval $[s, t]$. In our vectorial case, the set of admissible configurations Q is no longer convex, hence (4) has no longer a good sense and we must rely on the energetic formulation (5)–(6) as a natural generalization.

Mathematical advantage of the energetic formulation (5)–(6) by Mielke and Theil [16−18] is that it is free of time derivatives. The existence of thus defined *energetic solution* $(u, \nu) : [0, T] \to Q$ has been shown in [19], provided $\bar{G}$ is still

regularized by counting energy of possible spatial jumps in λ, as proposed in [20], p. 364.

For computational implementation, additional discretization of the set Q is necessary. The canonical approach is to apply P1-finite elements on a triangulation (with a discretization parameter h) of a polyhedral domain Ω for discretization u_h of u and elementwise constant (= homogeneous) so-called laminates (see [9]) to discretize ν. We implemented the *second-order laminate*, which leads to the four-atomic Young measure ν_h, where

$$\nu_h = \xi_{0h}\xi_{1h}\delta_{F_{1h}} + \xi_{0h}(1-\xi_{1h})\delta_{F_{2h}} + (1-\xi_{0h})\xi_{2h}\delta_{F_{3h}} + (1-\xi_{0h})(1-\xi_{2h})\delta_{F_{4h}}$$

with

$$F_{1h} = \nabla u_h - (1-\xi_{0h})a_h \otimes n_h - (1-\xi_{1h})a_{1h} \otimes n_{1h},$$
$$F_{2h} = \nabla u_h - (1-\xi_{0h})a_h \otimes n_h + \xi_{1h}a_{1h} \otimes n_{1h},$$
$$F_{3h} = \nabla u_h + \xi_{0h}a_h \otimes n_h - (1-\xi_{2h})a_{2h} \otimes n_{2h},$$
$$F_{4h} = \nabla u_h + \xi_{0h}a_h \otimes n_h + \xi_{2h}a_{2h} \otimes n_{2h}.$$

Here $0 \leq \xi_{ih} \leq 1$, $i = 0, 1, 2$, are elementwise constant. The vectors $a_{ih} \in \mathbb{R}^3$ and $n_{ih} \in \mathbb{R}^3$ are elementwise constant as well and, moreover, we may choose $|n_{ih}| = 1$. Hence, the whole Young measure ν_h is identified by means of ∇u_h and $\{\xi_{ih}, a_{ih}, n_{ih}\}$. This ensures that $(u_h, \nu_h) \in Q$. The same approximation was used, for instance, in [21,22].

In order to find an approximate energetic solution, we consider a fully-implicit time discretization based on the following incremental problem: take a time step $\tau > 0$ and let ν_h^0 be a given initial condition (we do not prescribe an initial condition for u_h because R depends only on ν), and, for $k = 1, ..., T/\tau \in \mathbb{N}$ we define recursively $(u_h^k, \nu_h^k)_{k=1,...,T/\tau}$ as a solution to the minimization problems

$$\left.\begin{array}{ll} \text{Minimize} & \bar{G}(k\tau, u_h, \nu_h) + R(\nu_h - \nu_h^{k-1}) \\ \text{subject to} & (u_h, \nu_h) \in Q \text{ with} \\ & \nu_h \text{ elementwise constant 2nd-order laminates.} \end{array}\right\} \quad (7)$$

3. COMPUTATIONAL EXPERIMENTS WITH CuAlNi

The *orthorhombic martensite* has 6 variants, i.e., counting also austenite, $L = 7$. The frame-indifferent stored energy composed of St. Venant–Kirchhoff-type materials for each (phase) variant is postulated as

$$\hat{\phi}(F) = \min_{\ell=0,...,6} \sum_{i,j,k,l=1}^{3} \frac{\varepsilon_{ij}^{\ell}\mathcal{C}_{ijkl}^{\ell}\varepsilon_{kl}^{\ell}}{2} + d_\ell, \quad \varepsilon^\ell = \frac{R_\ell^\top (U_\ell^\top)^{-1}F^\top F U_\ell^{-1}R_\ell - \mathbb{I}}{2}, \quad (8)$$

where $\mathcal{C}^\ell = \{\mathcal{C}_{ijkl}^\ell\}$ is the 4th-order tensor of elastic moduli, R_ℓ are rotation matrices relating the martensitic coordinates to the reference austenite, d_ℓ are some

offsets, and U_ℓ the distortion matrices: $U_0 = \mathbb{I}$ corresponds to austenite while

$$U_1 = \begin{pmatrix} \eta_2 & 0 & 0 \\ 0 & \eta_1 & \eta_3 \\ 0 & \eta_3 & \eta_1 \end{pmatrix}, \quad U_2 = \begin{pmatrix} \eta_1 & 0 & \eta_3 \\ 0 & \eta_2 & 0 \\ \eta_3 & 0 & \eta_1 \end{pmatrix}, \quad U_3 = \begin{pmatrix} \eta_1 & \eta_3 & 0 \\ \eta_3 & \eta_1 & 0 \\ 0 & 0 & \eta_2 \end{pmatrix}, \quad (9)$$

while the other three, i.e. $U_4, ..., U_6$, take $-\eta_3$ in place of η_3. An example of Cu-14.0wt%Al-4.2wt%Ni counts with $\eta_1 = 1.04245$, $\eta_2 = 0.9178$, and $\eta_3 = 0.01945$. The specific values of elastic moduli are determined from experiments; we refer to Sedlák et al. [23]. We also use the usual Voigt's notation, which (in a one-to-one way) replaces $\mathcal{C}^\ell$ by $\{\mathbb{C}_{ij}^\ell\}_{i,j=1}^6$. For $\ell = 0$, i.e. for austenite, by symmetry there are only 3 nonvanishing elastic moduli, i.e. here $\mathbb{C}_{11}^0 = \mathbb{C}_{22}^0 = \mathbb{C}_{33}^0 = 142.8$ GPa, $\mathbb{C}_{44}^0 = \mathbb{C}_{55}^0 = \mathbb{C}_{66}^0 = 93.5$ GPa, $\mathbb{C}_{12}^0 = \mathbb{C}_{23}^0 = \mathbb{C}_{13}^0 = 129.7$ GPa. The specific values for martensite (in the basis of a particular variant) are $\mathbb{C}_{11} = 189$ GPa, $\mathbb{C}_{22} = 141$ GPa, $\mathbb{C}_{33} = 205$ GPa, $\mathbb{C}_{44} = 54.9$ GPa, $\mathbb{C}_{55} = 19.7$ GPa, $\mathbb{C}_{66} = 62.6$ GPa, $\mathbb{C}_{12} = 124$ GPa, $\mathbb{C}_{13} = 45.5$ GPa, $\mathbb{C}_{23} = 115$ GPa. Matrices R_ℓ in (8) are proper rotations transforming $\mathbb{C}$ to the basis of austenite and can be found in [21]. The offset d_ℓ in (8) has been chosen as 3 MPa, which corresponds to the process temperature of 312 K.

As to the construction of the phase-indicator function $\mathcal{L} : \mathbb{R}^{3\times3} \to \mathbb{R}^7$, we take some $\delta > 0$ small and a smooth function $d : \mathbb{R} \to \mathbb{R}$ such that $d = 1$ in a neighbourhood of 0 and $d = \delta$ far from that neighbourhood, and put

$$\hat{\mathcal{L}}(F) := \left\{ \frac{d\big(\big|F^\top F - U_\ell^\top U_\ell\big|_{\mathrm{F}}^2\big)}{\sum_{l=0}^6 d\big(\big|F^\top F - U_l^\top U_l\big|_{\mathrm{F}}^2\big)} \right\}_{\ell=0}^6 . \quad (10)$$

The set K in (3) is chosen as a simplex in $\mathbb{R}^7$ and specific dissipation energies (or, equally, activation stresses) are set to be 2 MJ/m³ (= 2 MPa) for transformations between austenite and martensite and 1 Pa for transformations between various variants of martensite, which makes the so-called re-orientation of martensite almost nondissipative. It is an unfortunate reality that the data for the phenomenological dissipation model are very difficult to obtain. Moreover, dissipation mechanisms are often not fully autonomous and, e.g., may vary within the number of cycles in cyclical loadings. Here, the concrete value 2 MJ/m³ is approximately fitted with experiments reported in [24], fig. 1 or [25] fig. 4, while the value 1 Pa is to reflect that the reorientation of two martensite variants, which are rank-one connected, is nearly nondissipative at least if there are not much impurities in the material so that pinning effects are small (cf. also [26] for the case of austenite/martensite transformation).

4. RESULTS OF COMPRESSION TESTS

Our specimen is a block with dimensions $4\,\mathrm{mm} \times 9\,\mathrm{mm} \times 4\,\mathrm{mm}$, referring to the stress-free austenite Ω. Its bottom is fixed by the zero-displacement Dirichlet

boundary condition, while on its top we apply varying stress, ranging the interval $0 - 300$ MPa in the vertical direction (cf. Fig. 1). The initial condition is $\nu_h^0 = \delta_0$, i.e., the whole specimen is in the austenite. The form of stored energy (8) together with variants (9) reflect the case when the crystal lattice of austenite has the orientation (001). In many applications, however, the specimen is oriented differently, see e.g. [27]. Various material orientations can be easily implemented by using the specific stored energy $\bar{\phi}(F) = \hat{\phi}(FR_A)$, where R_A is a rotation of the austenite from (001). Four compression tests were performed for (0,tanα,1)-oriented single crystal with $\alpha = 0, 10, 20$, and 30 degrees (cf. Fig. 2).

It should be remarked that, in real CuAlNi single crystals, the 2H (γ_1') orthorhombic martensite, considered in the above text, occurs in compression tests near the (001) directions, while in directions closer to (011) or (111) another type of martensite, namely 18R (β_1') which is monoclinic, may be observed, too. To model it, other 12 wells would have to be included into the stored energy and other dissipation energies would have to be specified. Beside such expansion of the energies in the model, the simulations would expectedly be more difficult because the optimization algorithms are computationally less efficient if the landscape of the minimized energy in (7) has more local valleys. In the compression test presented here, the monoclinic martensite seems, indeed, relatively negligible, as documented in [25], fig. 5, and therefore we dared neglect it. Also, our aim has been rather to present the modelling aspects and the ability of the model itself.
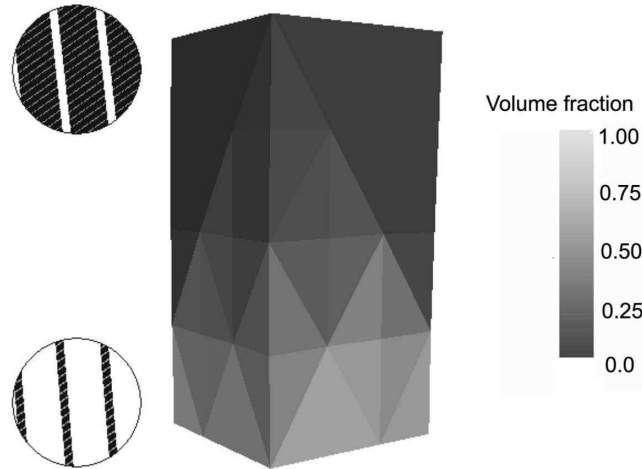

Fig. 1. Specimen, here (0,tan$10°$,1)-oriented CuAlNi single crystal, under compression loading at 200 MPa transforms from austenite (grey) to a twinned martensite (black) composed of two variants, namely U_1 and U_2, cf. (9). The austenite/twinned-martensite configuration reconstructed from computed Young measures is depicted on two chosen elements.
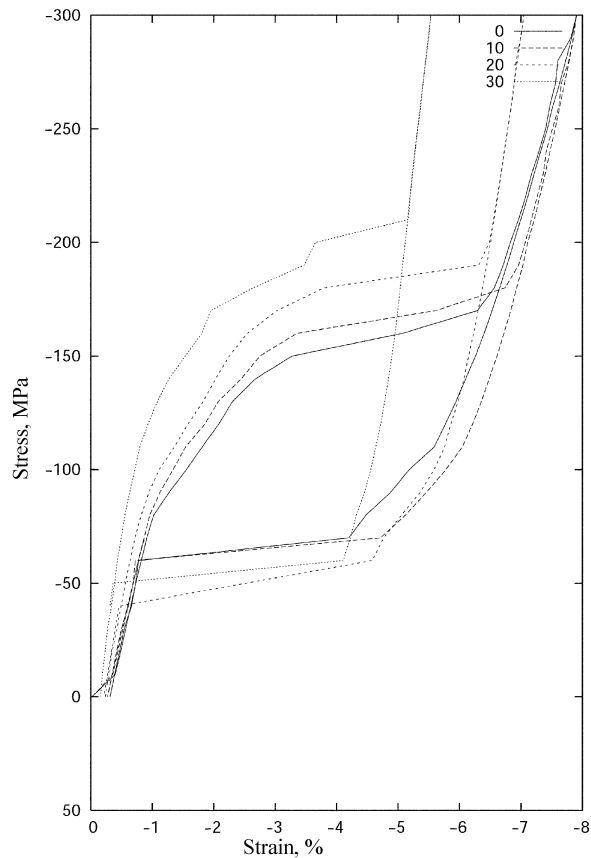
Fig. 2. Stress–strain response under cyclic compression load of a $(0,\tan\alpha,1)$-oriented single crystal depends substantially on α. Here $\alpha = 0°$, $10°$, $20°$, and $30°$ is depicted.

REFERENCES

1. Bhattacharya, K. *Microstructure of Martensite. Why it Forms and How it Gives Rise to the Shape-Memory Effect.* Oxford University Press, New York, 2003.
2. Frémond, M. and Miyazaki, S. *Shape Memory Alloys.* Springer, Wien, 1996.
3. James, R. D. and Hane, K. F. Martensitic transformations and shape-memory materials. *Acta Mater.*, 2000, **48**, 197–222.
4. Müller, S. Variational models for microstructure and phase transitions. In *Calculus of Variations and Geometric Evolution Problems* (Hildebrandt, S. et al., eds). *Lect. Notes in Math.*, 1999, **1713**, 85–210.

5. Otsuka, K. and Shimizu, K. Morphology and crystallography of thermoelastic Cu-Al-Ni martensite analyzed by the phenomenological theory. *Trans. Japan Inst. Metals*, 1974, **15**, 103–113.

6. Pitteri, M. and Zanzotto, G. *Continuum Models for Phase Transitions and Twinning in Crystals*. Chapman & Hall, Boca Raton, 2003.

7. Roubíček, T. Models of microstructure evolution in shape memory materials. In *Nonlinear Homogenization and its Application to Composites, Polycrystals and Smart Materials* (Ponte Castaneda, P., Telega, J. J. and Gambin, B., eds). Kluwer, Dordrecht, 2004, 269–304.

8. Ball, J. M. and James, R. D. Fine phase mixtures as minimizers of energy. *Archive Rat. Mech. Anal.*, 1988, **100**, 13–52.

9. Pedregal, P. *Parametrized Measures and Variational Principles*. Birkäuser, Basel, 1997.

10. Huo, Y. and Müller, I. Nonequilibrium thermodynamics of pseudoelasticity. *Continuum Mech. Thermodyn.*, 1993, **5**, 163–204.

11. Petryk, H. Thermodynamic conditions for stability in materials with rate-independent dissipation. *Phil. Trans. Roy. Soc. A*, 2005, **363**, 2479–2515.

12. Stupkiewicz, S. and Petryk, H. Modelling of laminated microstructures in stress-induced martensitic transformations. *J. Mech. Phys. Solids*, 2002, **50**, 2303–2331.

13. Thamburaja, P. and Anand, L. Polycrystalline shape-memory materials: effect of crystallographic texture. *J. Mech. Physics Solids*, 2001, **49**, 709–737.

14. Vivet, A. and Lexcelent, C. Micromechanical modelling for tension-compression pseudoelastic behaviour of AuCd single crystals. *Euro Phys. J. A. P.*, 1998, **4**, 125–132.

15. Levitas, V. I. The postulate of realizibility. *Int. J. Eng. Sci.*, 1995, **33**, 921–971.

16. Mielke, A. Evolution of rate-independent systems. In *Handbook of Differential Equations* (Dafermos, C. and Feireisl, E., eds). Elsevier, Amsterdam, 2005, 461–559.

17. Mielke, A. and Theil, F. On rate-independent hysteresis models. *Nonlin. Diff. Eq. Appl.*, 2004, **11**, 151–189.

18. Mielke, A., Theil, F. and Levitas, V. I. A variational formulation of rate-independent phase transform using an extremum principle. *Arch. Rat. Mech. Anal.*, 2002, **162**, 137–177.

19. Mielke, A. and Roubíček, T. Rate-independent model of inelastic behaviour of shape-memory alloys. *Multiscale Modeling Simul.*, 2003, **1**, 571–597.

20. Frémond, M. *Non-Smooth Thermomechanics*. Springer, Berlin, 2002.

21. Kružík, M., Mielke, A. and Roubíček, T. Modelling of microstructure and its evolution in SMA single-crystals, in particular in CuAlNi. *Meccanica*, 2005, **40**, 389–418.

22. Roubíček, T. and Kružík, M. Mesoscopic model of microstructure evolution in shape memory alloys, its numerical analysis and computer implementation. *GAMM Mitteilungen*, 2006, **29**, 192–214.

23. Sedlák, P., Seiner, H., Landa, M., Novák, V., Šittner, P. and Mañosa, L. l. Elastic constants of bcc austenite and 2H orthorhombic martensite in CuAlNi shape memory alloy. *Acta Mater.*, 2005, **53**, 3643–3661.

24. Novak, V., Šittner, P. and Zárubová, N. Anisotropy of transformation characteristics of Cu-base alloys. *Mater. Sci. Eng. A*, 1997, **234–236**, 414–417.

25. Novak, V., Šittner, P., Vokoun, D. and Zárubová, N. On the anisotropy of martensitic transformation in Cu-based alloys. *Mater. Sci. Eng. A*, 1999, **273–275**, 280–285.

26. James, R. D. and Zhang, Z. A way to search for multiferroic materials with "unlikely" combination of physical properties. In *Magnetism and Structure in Functional Materials*, Ch. 9 (Planes, A., Manoza, L. and Saxena, A., eds). Springer, 2005, 159–176.

27. Novak, V., Šittner, P., Ignacová, S. and Černoch, T. Transformation behavior of prism shaped shape memory alloy single crystals. *Mater. Sci. Eng. A*, 2006, **438–440**, 755–762.

Kujumäluga sulamite mesoskoopiline mudel

Tomáš Roubíček, Martin Kružík ja Jan Koutný

On kasutatud austeniit- ja eriti martensiitfaaside multimiinimumidega energia-potentsiaali mõistet ja dissipatiivse pseudopotentsiaali kontseptsiooni kujumäluga sulamite isotermilisuse tasemest sõltumatu martensiitse ülemineku mesoskoopilise mudeli koostamiseks. On üle vaadatud teoreetilised tulemused, mis käsitlevad laminaatidega seotud Youngi mõõdete numbrilist lähendamist, ja esitatud numb-rilise simulatsiooni tulemused CuAlNi monokristallide jaoks.